

Kinetic scheme of biomass pyrolysis considering secondary charring reactions

Andrés Anca-Couce ^{a,*}, Ramin Mehrabian ^{a,b}, Robert Scharler ^{a,b,c}, Ingwald Obernberger ^{a,b,c}

^a Institute for Process and Particle Engineering, Graz University of Technology, Inffeldgasse 21b, 8010 Graz, Austria

^b BIOENERGY 2020+ GmbH, Inffeldgasse 21b, 8010 Graz, Austria

^c BIOS BIOENERGIESYSTEME GmbH, Inffeldgasse 21b, 8010 Graz, Austria



ARTICLE INFO

Article history:

Received 9 May 2014

Accepted 22 July 2014

Keywords:

Pyrolysis

Charring

Kinetics

Secondary

ABSTRACT

A widely applicable kinetic scheme for pyrolysis is still missing. In this work an adaptation of the mechanistic scheme developed by Ranzi et al. (2008) for pyrolysis of small ash free biomass particles is proposed. The scheme is modified to include secondary char formation reactions, which are relevant for particles of a certain thickness, and sugar formation is avoided due to the catalytic effect of alkali metals in biomass. The predictions of the adapted scheme are compared to experimental data from the literature of pyrolysis in fixed beds of particles with a size of around 1 cm. It is shown that the adaptation improves the prediction of the final char yield and its CHO composition and also the yields of the main groups of volatiles, as carbonyls + alcohols, sugars and water vapor.

© 2014 Elsevier Ltd. All rights reserved.

1. Introduction

Biomass, as other renewable energy sources, is expected to play a more important role in the energy mix of the future. Pyrolysis is a promising conversion process by itself to generate liquid bio-fuel and bio-char and also a main sub-process in other thermal conversion processes as gasification, combustion, smouldering or hydro-thermal carbonization. To describe these processes in different reactor configurations, where transport phenomena are coupled with chemical reactions [1], accurate kinetics of biomass pyrolysis which can provide the final product composition are required. However, pyrolysis of biomass proceeds via a very complex set of competitive and concurrent reactions. The exact mechanism remains unknown [2] and a widely applicable kinetic scheme for pyrolysis is still missing.

Many of the available pyrolysis schemes were reviewed by Di Blasi [3]. Schemes can be categorized into single component and multi-component. In single-component schemes the final products are usually lumped into 3 categories: solid (char), liquid (tar) and gas, although there is a high heterogeneity in each category. Examples of main liquid components are water, pyrolytic lignin or acetic acid, which have very different properties. Pyrolysis is described as the competition between formation of each lumped product. This

scheme attempts to be able to predict the product distribution at a different range of conditions, ranging from slow to fast heating rate, and it is the most commonly employed to describe the kinetics of biomass pyrolysis in single particle and reactor models. In this scheme the primary tar can further react in a secondary exothermic reaction to produce more permanent gases or secondary char.

In the multi-component schemes there are usually 3 components representing the main biomass components: cellulose, hemi-cellulose and lignin. In this scheme usually each component is represented with one reaction and just the mass loss evolution is predicted, without giving information about the product composition. Sometimes fixed yields of products are assumed for each component, based on experimental data [4]. In Miller and Bellan [5] a competitive scheme between char, tar and gas formation is proposed for each biomass component. But none of these single-component or multi-component schemes are mechanistic and provide a detailed product composition.

For individual compounds as cellulose [6,7] or lignin [8,9] mechanistic schemes were proposed based on the analysis of the several reaction mechanisms rather than a global approach. A mechanistic scheme was proposed for biomass by Ranzi et al. [10], considering biomass as formed by cellulose, hemi-cellulose and 3 types of lignin and 20 representative species are considered to describe the volatiles. The product composition provided by this scheme was partially validated with data obtained from fast pyrolysis of small ash free biomass particles and the mass loss

* Corresponding author. Tel.: +43 (0) 316 873 30432; fax: +43 (0) 316 873 1030432.

E-mail address: anca-couce@tugraz.at (A. Anca-Couce).

evolution from micro-TGA experiments, i.e., conditions where secondary reactions are minimized.

However there is no mechanistic scheme available for pyrolysis when secondary reactions are not negligible. Secondary reactions are present in particles of a certain thickness when there is enough residence time of the volatiles during char formation and this is the case for most of the pyrolysis processes in fixed or fluidized beds, and other processes where pyrolysis is present, as combustion or gasification. The presence of inorganics in the feedstock also promotes secondary reactions [3]. The nature of these reactions is explained in detail in Section 2. The focus of this work is to propose an adaptation of the Ranzi et al. [10] scheme based on the literature to improve the predictions of the pyrolysis product composition when secondary charring reactions are relevant. The predictions of the adapted scheme are compared to experimental data for model validation.

2. Pyrolysis mechanism

2.1. Cellulose

The cellulose pyrolysis mechanism from Ranzi et al. [10], schematically summarized in Fig. 1a and detailed in Table 1, is based on the scheme of Piskorz et al. [11]. Cellulose can be converted to active cellulose without appreciable mass loss through R1 or converted to char and water through R4. Reaction R1 is always the prevalent reaction in this competition, although the proportion of R4 is higher at low temperatures (due to lower activation energy), leading to higher char yields at low temperatures. When active

cellulose is formed, it is almost instantaneously consumed either through the ring fragmentation (R2) or the transglycosylation (R3) pathways. In the first one several low molecular weight species are produced, including carbonyls, furans and permanent gases, together with char. In the second just a sugar, i.e. levoglucosan (LVG), is produced. At low temperatures the production of LVG is dominating. At 400 °C more than 90% of the active cellulose is converted to LVG. This percentage is even higher at lower temperatures.

It is worth noting that the original scheme developed by Ranzi et al. [10] does not consider the influences of inorganics and secondary charring reactions. This scheme was developed for pure ash free cellulose, but the presence of ash, especially alkali metals, strongly catalyzes the fragmentation pathway (R2) over transglycosylation (R3) [12,13]. To give some numbers, Patwardhan et al. [14] reported a 60% levoglucosan yield for pyrolysis of very small samples of ash free cellulose at 500 °C (similar to the prediction of the model). But with the addition of just 1% ash, the levoglucosan yield decreased to a value lower than 20%. About char formation, it should be stated that char formation from cellulose is not a primary step but a result of secondary reactions in the gas and solid phases, as stated by the reviews of several authors [12,13,15]. Mass transfer of the volatiles out of the sample matrix after devolatilization plays a main role. If the volatiles cannot escape from the matrix they undergo charring. So anything that hinders mass transport increases charring [16,17]. This can be shown by comparing the TGA experiments of Antal and Varhegyi [12] that were done in an open sample holder with 1 mg of cellulose, where the final char yield was 5%, to experiments that have

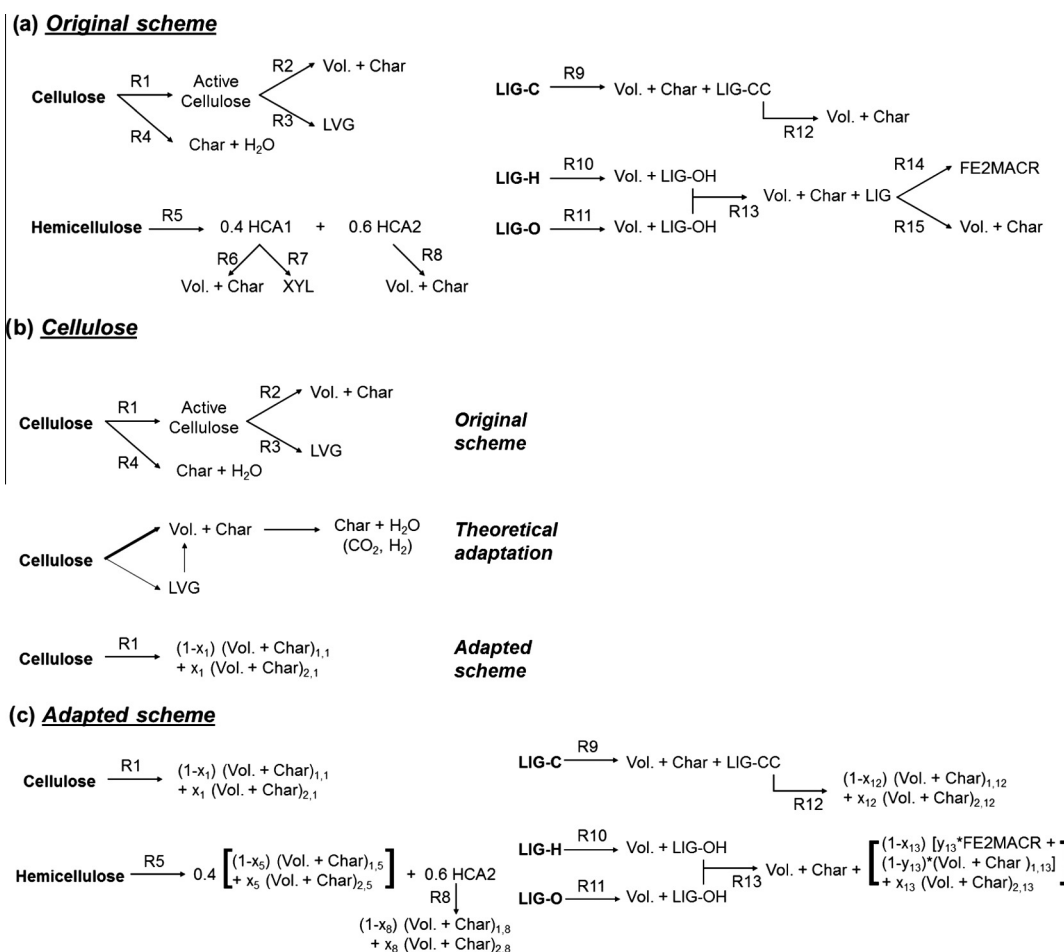


Fig. 1. Reaction schemes. (a) Original scheme from Ranzi et al. [10]. (b) Adaptation for cellulose. (c) Adapted scheme.

Table 1

Reactions of original scheme from Ranzi et al. [10], as reported by Blondeau and Jeanmart [41].

Reaction		A (s^{-1})	E (kJ/mol)
1	CELL → CELLA	8×10^{13}	192.5
2	CELLA → 0.95 HAA + 0.25 GLYOX + 0.2 CH ₃ CHO + 0.25 HMFU + 0.2 C ₃ H ₆ O + 0.16 CO ₂ + 0.23 CO + 0.9 H ₂ O + 0.1 CH ₄ + 0.61 Char	1×10^9	125.5
3	CELLA → LVG	4T	41.8
4	CELL → 5 H ₂ O + 6 Char	8×10^7	133.9
5	HCE → 0.4 HCEA1 + 0.6 HCEA2	1×10^{10}	129.7
6	HCEA1 → 0.75 G{H ₂ } + 0.8 CO ₂ + 1.4 CO + 0.5 CH ₂ O + 0.25 CH ₃ OH + 0.125 ETOH + 0.125 H ₂ O + 0.625 CH ₄ + 0.25 C ₂ H ₄ + 0.675 Char	3×10^9	113.0
7	HCEA1 → XYL	3T	46.0
8	HCEA2 → 0.2 CO ₂ + 0.5 CH ₄ + 0.25 C ₂ H ₄ + 0.8 G{CO ₂ } + 0.8 G{COH ₂ } + 0.7 CH ₂ O + 0.25 CH ₃ OH + 0.125 ETOH + 0.125 H ₂ O + Char	1×10^{10}	138.1
9	LIG-C → 0.35 LIG-CC + 0.1 pCOUMARYL + 0.08 PHENOL + 0.41 C ₂ H ₄ + H ₂ O + 0.495 CH ₄ + 0.32 CO + G{COH ₂ } + 5.735 Char	4×10^{15}	202.9
10	LIG-H → LIG-OH + C ₃ H ₆ O	2×10^{13}	156.9
11	LIG-O → LIG-OH + CO ₂	1×10^9	106.7
12	LIG-CC → 0.3 pCOUMARYL + 0.2 PHENOL + 0.35 C ₃ H ₄ O ₂ + 0.7 H ₂ O + 0.65 CH ₄ + 0.6 C ₂ H ₄ + G{COH ₂ } + 0.8 G{CO} + 6.4 Char	5×10^6	131.8
13	LIG-OH → LIG + H ₂ O + CH ₃ OH + 0.45 CH ₄ + 0.2C ₂ H ₄ + 1.4 G{CO} + 0.6 G{COH ₂ } + 0.1 G{H ₂ } + 4.15 Char	3×10^8	125.5
14	LIG → FE2MACR	8T	50.2
15	LIG → H ₂ O + 0.5 CO + 0.2 CH ₂ O + 0.4 CH ₃ OH + 0.2 CH ₃ CHO + 0.2 C ₃ H ₆ O + 0.6 CH ₄ + 0.65 C ₂ H ₄ + G{CO} + 0.5 G{COH ₂ } + 5.5 Char	1.2×10^9	125.5
16	G{CO ₂ } → CO ₂	1×10^5	100.4
17	G{CO} → CO	1×10^{13}	209.2
18	G{COH ₂ } → CO + H ₂	5×10^{11}	272.0
19	G{H ₂ } → H ₂	5×10^{11}	313.8

been done with the addition of a cover (with a small pinhole) to the sample pan, where the char yield increased to 19%. It is known that char yields increase at low heating rates/temperatures. But residence time of the volatiles is reported to be more important in determining the char yield than the temperature/heating rate. This may correspond to a quite low activation energy of the char formation reaction, where the reaction rate is less temperature dependent [17].

The proposed adaptation of the scheme for cellulose is shown schematically in Fig. 1b and detailed in Table 2. Cellulose pyrolysis is described with just one reaction representing devolatilization plus an inclusion of a secondary reaction representing charring. The kinetics of this devolatilization reaction are the kinetics of the reaction to produce active cellulose (R1) in the original scheme. But, as seen in Fig. 1b, this reaction would directly produce the fragmentation products [(Vol. + Char)_{1,1}, which are the products of R2 in the original scheme], charring products [(Vol. + Char)_{2,1}] and no LVG (product of R3 in the original scheme). The fragmentation products of primary pyrolysis of cellulose are named (Vol. + Char)_{1,1} in Fig. 1b as they are the primary volatiles and char produced in reaction R1. The product composition of this fragmentation, i.e., the composition of (Vol. + Char)_{1,1}, is detailed in Table 2. Cellulose produces (in mols) 0.95 HAA + 0.25 GLYOX + 0.2

CH₃CHO + 0.25 HMFU + 0.2 C₃H₆O + 0.16 CO₂ + 0.23 CO + 0.9 H₂O + 0.1 CH₄ + 0.61 Char. The produced primary volatiles include several low molecular weight compounds which are classified in groups in Table 3. It has been shown that the presence of minerals in biomass favors the fragmentation pathway over LVG formation. The LVG pathway may also be followed in biomass pyrolysis, but in a much minor proportion than the other one and some of the LVG would later fragment in secondary reactions, as seen in Fig. 1b. The product composition of R2 is a good initial guess for the product composition of LVG fragmentation reaction. Therefore, assuming that this devolatilization reaction just produces the fragmentation products and no LVG is reasonable. The previous char formation reaction at low temperatures (R4) is now not considered. To neglect this reaction considering char as a secondary product was also proposed by Lin et al. [15]. There is, however, an extension of reaction R1 representing this secondary char formation in the adapted scheme. The new products are named in Fig. 1b (Vol. + Char)_{2,1} as they are secondary volatiles and char produced in reaction R1. The amount of this reaction depends, in theory, on the temperature (more charring at low temperatures, lower activation energy) but mainly on the retention time and partial pressure of the volatiles that undergo the charring reactions. Also the presence of minerals in biomass is known to catalyze

Table 2

Reactions of adapted scheme.

Reaction		A (s^{-1})	E (kJ/mol)
1	CELL → (1 - x ₁) * (0.95 HAA + 0.25 GLYOX + 0.2 CH ₃ CHO + 0.25 HMFU + 0.2 C ₃ H ₆ O + 0.16 CO ₂ + 0.23 CO + 0.9 H ₂ O + 0.1 CH ₄ + 0.61 Char + x ₁ * (5.5 Char + 4 H ₂ O + 0.5 CO ₂ + H ₂)	8×10^{13}	192.5
5	HCE → 0.4 * [(1 - x ₅) * (0.75 G{H ₂ } + 0.8 CO ₂ + 1.4 CO + 0.5 CH ₂ O + 0.25 CH ₃ OH + 0.125 ETOH + 0.125 H ₂ O + 0.625 CH ₄ + 0.25 C ₂ H ₄ + 0.675 Char) + x ₅ * (4.5 Char + 3 H ₂ O + 0.5 CO ₂ + H ₂)] + 0.6 HCEA2	1×10^{10}	129.7
8	HCEA2 → (1 - x ₈) * (0.2 CO ₂ + 0.5 CH ₄ + 0.25 C ₂ H ₄ + 0.8 G{CO ₂ } + 0.8 G{COH ₂ } + 0.7 CH ₂ O + 0.25 CH ₃ OH + 0.125 ETOH + 0.125 H ₂ O + Char + x ₈ * (4.5 Char + 3 H ₂ O + 0.5 CO ₂ + H ₂)	1×10^{10}	138.1
9	LIG-C → 0.35 LIG-CC + 0.1 pCOUMARYL + 0.08 PHENOL + 0.41 C ₂ H ₄ + H ₂ O + 0.495 CH ₄ + 0.32 CO + G{COH ₂ } + 5.735 Char	4×10^{15}	202.9
10	LIG-H → LIG-OH + C ₃ H ₆ O	2×10^{13}	156.9
11	LIG-O → LIG-OH + CO ₂	1×10^9	106.7
12	LIG-CC → (1 - x ₁₂) * (0.3 pCOUMARYL + 0.2 PHENOL + 0.35 C ₃ H ₄ O ₂ + 0.7 H ₂ O + 0.65 CH ₄ + 0.6 C ₂ H ₄ + G{COH ₂ } + 0.8 G{CO} + 6.4 Char) + x ₁₂ * (14.5 Char + 3 H ₂ O + 0.5 CO ₂ + 4 H ₂)	5×10^6	131.8
13	LIG-OH → H ₂ O + CH ₃ OH + 0.45 CH ₄ + 0.2C ₂ H ₄ + 1.4 G{CO} + 0.6 G{COH ₂ } + 0.1 G{H ₂ } + 4.15 Char + [(1 - x ₁₃) * (y ₁₃ * FE2MACR + (1 - y ₁₃) * (H ₂ O + 0.5 CO + 0.2 CH ₂ O + 0.4 CH ₃ OH + 0.2 CH ₃ CHO + 0.2 C ₃ H ₆ O + 0.6 CH ₄ + 0.65 C ₂ H ₄ + G{CO} + 0.5 G{COH ₂ } + 5.5 Char)) + x ₁₃ * (10.5 Char + 3 H ₂ O + 0.5 CO ₂ + 3 H ₂)]	3×10^8	125.5
16	G{CO ₂ } → CO ₂	1×10^5	100.4
17	G{CO} → CO	1×10^{13}	209.2
18	G{COH ₂ } → CO + H ₂	5×10^{11}	272.0
19	G{H ₂ } → H ₂	5×10^{11}	313.8

Table 3
List of species.

Abbreviation	Name	Atomic composition	Group
<i>Solids</i>			
CELL	Cellulose	C ₆ H ₁₀ O ₅	
CELLA	Activated cellulose	C ₆ H ₁₀ O ₅	
HCE	Hemicellulose	C ₅ H ₈ O ₄	
HCEA1	Activated hemicellulose 1	C ₅ H ₈ O ₄	
HCEA2	Activated hemicellulose 2	C ₅ H ₈ O ₄	
LIG	Lignin	C ₁₁ H ₁₂ O ₄	
LIG-C	Carbon-rich lignin	C ₁₅ H ₁₄ O ₄	
LIG-H	Hydrogen-rich lignin	C ₂₂ H ₂₈ O ₉	
LIG-O	Oxygen-rich lignin	C ₂₀ H ₂₂ O ₁₀	
LIG-CC	Carbon-rich lignin 2	C ₁₅ H ₁₄ O ₄	
LIG-OH	OH-rich lignin	C ₁₉ H ₂₂ O ₈	
G(CO ₂)	Trapped CO ₂	CO ₂	
G(CO)	Trapped CO	CO	
G(COH ₂)	Trapped COH ₂	CH ₂ O	
G(H ₂)	Trapped H ₂	H ₂	
Char	Char	C	
<i>Volatiles</i>			
HAA	Hydroxyacetraldehyde (Acetic acid)	C ₂ H ₄ O ₂	Carbonyls + alcohols
GLYOX	Glyoxal	C ₂ H ₂ O ₂	Carbonyls + alcohols
C ₃ H ₆ O	Propanal (Acetone)	C ₃ H ₆ O	Carbonyls + alcohols
C ₃ H ₄ O ₂	Propanedial	C ₃ H ₄ O ₂	Carbonyls + alcohols
HMFU	5-hydroxymethyl-furfural	C ₆ H ₆ O ₃	Furans
LVG	Levoglucosan	C ₆ H ₁₀ O ₅	Sugars
XYL	Xylose monomer	C ₅ H ₈ O ₄	Sugars
pCOUNARYL	Paracoumaryl alcohol	C ₉ H ₁₀ O ₂	Phenolics
PHENOL	Phenol	C ₆ H ₆ O	Phenolics
FE2MACR	Sinapaldehyde	C ₁₁ H ₁₂ O ₄	Phenolics
H ₂	Hydrogen	H ₂	Permanent gases
CO	Carbon monoxide	CO	Permanent gases
CO ₂	Carbon dioxide	CO ₂	Permanent gases
CH ₄	Methane	CH ₄	Permanent gases
CH ₂ O	Formaldehyde	CH ₂ O	Carbonyls + alcohols
CH ₃ OH	Methanol	CH ₄ O	Carbonyls + alcohols
C ₂ H ₄	Ethylene	C ₂ H ₄	Permanent gases
CH ₃ CHO	Acetaldehyde	C ₂ H ₄ O	Carbonyls + alcohols
ETOH	Ethanol	C ₂ H ₆ O	Carbonyls + alcohols
H ₂ O	Water vapor	H ₂ O	Water vapor

significantly these charring reactions [3]. Therefore, an Arrhenius expression, which just shows the influence of temperature, is not employed but an adjustable parameter “ x_1 ”. This parameter represents the amount of secondary charring reactions, that is, the amount of the initial fragmentation primary products – (Vol. + Char)_{1,1} – that will further react to form the secondary products – (Vol. + Char)_{2,1} –. This parameter should depend on all the previous variables, as retention time, partial pressure, presence of minerals and temperature.

It should be mentioned that this adaptation does not significantly affect the mass loss evolution for the typical heating rates in particles of a certain thickness. It just modifies the final char yield prediction. In the original scheme, when the active cellulose is produced, it is almost instantaneously consumed through one of the two pathways at low or medium heating rates. At higher heating rates there is a delay between the production and decomposition of active cellulose. At a constant heating rate of 20 K/s, active cellulose is decomposed around 0.3 s later than its production, i.e., with a delay of just 6 °C. This is a typical heating rate in fluidized bed conditions. For fixed bed conditions, heating rates are usually lower. Therefore, the adaptation, which eliminates reactions R2 and R3, does not significantly affect the mass loss evolution for typical fixed or fluidized bed conditions. Moreover, it was stated that TGA experiments from cellulose can be completely

determined with one single reaction, without the need of competitive reactions [18]. It was postulated by Mamleev et al. [19] that both the fragmentation and transglycosylation reactions at typical heating rates of thermogravimetry are almost merged in one reaction.

In the secondary charring reaction not just H₂O is produced together with char, but also CO₂ and H₂. These products were also proposed by Milosavljevic et al. [17] and Vinu et al. [6]. The stoichiometry of the products of this charring reaction, that is, the product composition of (Vol. + Char)_{2,1}, is detailed in Table 2 and determined based on the micro-TGA experiments of Jensen et al. [20] with normal and washed straw. With washed straw, where much less secondary reactions are present, around 10% less water and char (in mass related to dry biomass) are produced, and around 5% less CO₂. The reported decrease of CO and CH₄ was much lower. Therefore, in the secondary reaction the mass production of H₂O and char would be similar, and higher than the CO₂ production. This trend is confirmed by the micro-TGA experiments of Gomez et al. [21] with untreated and washed wood (pine and beech). The reduction of the char and H₂O yields is in the range 2–3% (in mass related to dry biomass). For CO₂, it is in the range 0.8–1.4% and for CO lower than 0.5%. Therefore, the trend is valid for lignocellulosic biomass in general. The stoichiometric factors are selected to fulfil approximately these conditions. The elemental balance is closed with H₂.

Finally, it should be mentioned that some char is already produced in R1, the primary pyrolysis reaction, as one of the original fragmentation products. This case, where the “ x_1 ” parameter representing the amount of secondary charring reactions is equal to 0, should be considered as representative of conditions with a low amount of secondary reactions. When more charring reactions are present, the “ x_1 ” parameter increases.

2.2. Hemicellulose and lignin

The original scheme of hemicellulose is a two-step scheme (Fig. 1a). Hemicellulose first decomposes without mass loss in two different types of active hemicellulose, 1 and 2. The decomposition of the first active hemicellulose 1 (HCA1) resembles the one of cellulose, as it is decomposed in a competition between the formation of a sugar (XYL in R7) and a fragmentation pathway (R6). Also HCA1, as active cellulose, is almost instantaneously consumed when it is produced for the typical heating rates of this study. Then, HCA2 is decomposed with some delay after the decomposition of HCA1. The hemicellulose scheme is based on pyrolysis of xylan, which is a good representative for hemicelluloses of hardwoods. Pyrolysis of xylan can be described with two successive reactions, contrary to cellulose where one reaction is enough to describe it [22].

Information about pyrolysis of hemicellulose is scarce in the literature, but due to the similarities to cellulose, the adaptation of the scheme is made following the same principles as for the adaptation of the cellulose scheme. As seen in summarized scheme of Fig. 1c, the competition between R6 (fragmentation) and R7 (sugar formation) is eliminated and just the fragmentation pathway is followed. The primary volatiles and char produced in reaction R5 are named (Vol. + Char)_{1,5} in Fig. 1c. The secondary charring products (Vol. + Char)_{2,5}, produced from the previous fragmentation products, are considered through the parameter “ x_5 ”. The product composition of (Vol. + Char)_{1,5} and (Vol. + Char)_{2,5} are detailed in Table 2. In the decomposition of HCA2, through R8, the presence of secondary reactions are also considered by the parameter “ x_8 ”.

The original scheme of lignin consists of three different components: LIG-C, LIG-H and LIG-O, which are richer in carbon, hydrogen and oxygen, respectively. Lignin decomposition occurs in several steps, which corresponds to the broad temperature range

of the lignin decomposition. LIG-C decomposes in reaction R9, giving LIG-CC as an intermediate solid product which further reacts in R12. Decomposition of both LIG-H and LIG-O produce LIG-OH, which further decompose, in R13. One of the products of R13 is LIG. Its decomposition scheme resembles the schemes of cellulose and hemicellulose, as it reacts almost instantaneously in a competition between a phenolic (FE2MACR, R14) and a fragmentation pathway (R15).

The modifications are done in the decomposition of LIG-OH and LIG-CC. The LIG component resembles the active components in the previous schemes. But, in the modification, the production of FE2MACR is not eliminated, as done with sugars. This compound represents several phenolic compounds, which are produced in significant amounts at the presence of minerals and secondary charring reactions [8]. The proportions of FE2MACR and the fragmentation pathways are kept the same as in the original scheme with a polynomial interpolation that describes the production of FE2MACR from LIG as a function of temperature, y_{13} in Table 2. The products of secondary charring reactions, which are produced from both the fragmentation products and FE2MACR, are named as (Vol. + Char)_{2,13} in the modified scheme. The secondary reactions are also included in reaction R12 from LIG-CC.

As in the case of cellulose, the elimination of reactions R6, R7, R14 and R15 in the adapted scheme does not significantly affect the mass loss evolution, just the final char yield and product composition. In the original scheme char is not just produced as pure carbon, but also as several G{} forms (G{CO₂}, G{CO}, G{COH₂}) and G{H₂}) which further react at higher temperatures producing CO₂, CO or H₂. It represents the further char devolatilization that occurs at high temperatures. These reactions are kept in the adapted scheme.

It should be also mentioned that there is a high scattering for the activation energies of the biomass components in multi-component schemes in the literature, as reviewed by Anca-Couce et al. [23]. But the dominating activation energies of the current scheme (192 kJ/mol for cellulose, 129.7 and 138.1 for hemicellulose and 202.9, 131.8 and 125.5 for lignin) are in the range of values supported by the application of isoconversional methods describing TGA experiments [23]. Activation energies of around 200 kJ/mol are supported by isoconversional methods for cellulose. Lower values than for cellulose, but higher than 100 kJ/mol, are supported for hemicellulose. Also for lignin high values of the activation energy are supported by isoconversional methods and not the very low activation energies (<50 kJ/mol) that are usually reported in the literature. This fact and the good prediction of micro-TGA data by the original scheme shown in Frassoldati et al. [24], lead to focus for the adaptation on the reaction products without modification of the reaction kinetics (E and A values), as the mass loss predictions of the scheme are already precise.

3. Results and discussion

3.1. Experimental and model results

Experimental data from literature concerning product compositions from fixed-bed pyrolysis with particles of a few mm or cm was collected for model validation. A complete characterization of the product composition is difficult to find, due to the difficulties of measuring the very different products from pyrolysis, as different techniques are required. The works of Branca et al. [25] and Milhe et al. [26] were employed, as they provide a very comprehensive characterization.

The pyrolysis experiments of Branca et al. [25] were done in a batch process in a cylindrical reactor of 6.3 cm internal diameter that is placed in a furnace and where preheated N₂ is introduced from the top. A mass of 180 g pre-dried beech wood particles

was fed in the reactor, resulting in an initial height of the reactor of 15 cm. The beech particles were parallelepipeds with particle sizes from 5 to 20 mm with an ash content of 0.5% d.b. In the experiments of Milhe et al. [26] pine wood chips with particle sizes of 3–13 mm with an ash content of 0.4% d.b were fed continuously into a cylindrical reactor of 20 cm internal diameter. The bed has a height of 45 cm and two propane burners provide combusted gases at high temperatures to achieve the pyrolysis temperatures. In both experiments the volatiles go through a condensation system. The water content is measured by Karl-Fisher titration and pyrolysis liquids are analyzed by GC/MS. The permanent gases are also measured.

The two experiments from Mihle et al. [26] performed at 375° and 475 °C, and the experiment from Branca et al. [25] at 527 °C are selected for a comparison to the pyrolysis model. The batch experiment of Branca et al. [25] is modeled with a constant heating rate of 30 K/min until the final temperature of 527 °C without retention time at the final temperature, as reported in that work. The continuous experiments of Mihle et al. [26] are modeled assuming a constant temperature of 375 or 475 °C during 28 min. The heat-up phase is assumed to occur very fast. The retention time is calculated based on the bed height and solid fuel feeding rate reported in that work, and a dry bulk density of 175 kg/m³ [27].

The initial composition of the two different biomass types are in mass percentage: 46.4% CELL, 30.9% HCE, 4.3% LIG-C, 9.2% LIG-H and 9.2% LIG-O for beech; 45.0% CELL, 28.0% HCE, 7.0% LIG-C, 10.0% LIG-H and 10.0% LIG-O for pine. Values for beech, employed in the experiments from Branca et al. [25], are adapted from Di Blasi et al. [28] and values for pine, employed in the experiments from Mihle et al. [26], are taken from Frassoldati et al. [24]. The original and adapted kinetic schemes are applied with the described heating programs and an explicit method with a time step of 0.1 ms. At each time step, the reaction rate coefficients are calculated with the expression $k = A \exp(-E/RT)$ [1/s]. The pre-exponential factor A and activation energy E for each reaction were presented in Tables 1 and 2 and the employed temperature is the one at the beginning of the time step. The reaction rates are then calculated employing the solid concentrations at the beginning of the time step. The new solid composition at the end of the time step is obtained with this explicit approach and the released masses during the time step of the 20 volatiles species are calculated. The calculations are performed in Matlab. The final product composition predicted by the models is compared to the measured values. Mass loss evolutions are not compared as the model is purely kinetic. Heat and mass transfer limitations, which are present in fixed beds and affect the mass loss evolution over time, are not described by the model.

Experiments were chosen in the temperature range of roughly ≤500 °C, because at these temperatures homogeneous tar cracking reactions are minimized, as shown by Gomez-Barea and Leckner [29], where considering several tar cracking kinetics from the literature and a retention time of 0.5 s, the tar conversion for all tar components was below 10% w.t. This does not mean that there are not tar reactions at these low temperatures, as heterogeneous tar cracking occurs at lower temperatures, around 400 °C [30,31]. Actually tar cracking may be one of the reactions involved in charring, and the distinction between these two reaction types is not really clear. But there are some differences in the global product composition of these reactions. While homogenous tar cracking at high temperatures produces mainly CO and H₂ [32,33], in charring reactions H₂O, char and also CO₂ are the main products, as previously reviewed. In this work homogeneous tar cracking reactions are not considered.

The results from the original and adapted schemes are compared to the experimental data. The results are provided in Table 4,

where the “ x ” parameters representing the amount of secondary charring reactions in the adapted scheme have a constant value of 0.3 for all reactions. Later on, in Section 3.2, it is analyzed how variations in the “ x ” parameters affect the results.

To make the comparison between model and experiments, the condensable species are classified in six main groups (see Tables 3 and 4), depending of the chemical structure and functional groups: carbonyls + alcohols, furans, sugars, phenolics, BTX/PAH and water vapor. The carbonyl + alcohol group includes several aldehydes, ketones, carboxylic acids and alcohols. Sugars are produced from cellulose and hemicellulose, being levoglucosan the main example. Furans, heterocyclic compounds, are also reported to be produced mainly by cellulose and also by hemicellulose. On the other hand phenolics are aromatic compounds with a phenyl group (e.g. guaiacols, syringols, cresols, catechols or phenols) and have mainly a lignin origin. BTX/PAH are aromatics with one (BTX) or several rings (PAH) but, as opposite to phenolics, without oxygen content. The species in each group have usually properties in the same range, as it is the case for heat of reaction or boiling temperature.

Not all the condensable species could be detected in the experimental results. The detected compounds, after condensation in bio-oil, are:

- Water, detected by Karl–Fisher titration.
- Organic species, detected by GC/MS. They include several carbonyls, alcohols, furans, phenolics, BTX/PAH and levoglucosan.

The non-detected liquids could be liquids that are not condensed or that cannot be detected by CG/MS. Liquids that cannot be detected by GC/MS include non-volatile compounds that could be characterized by HPLC and pyrolytic lignin. Pyrolytic lignin is composed of aromatic compounds with a phenolic structure and more than one aromatic ring. By GC/MS just phenolics with one aromatic ring are detected (named as Exp. 1 ring in Table 4). Phenolics with more aromatic rings form pyrolytic lignin and cannot be detected by GC/MS.

Therefore, assumptions are needed to classify the non-detected liquids. It was assumed that 15% of the total liquids correspond to pyrolytic lignin. Pyrolytic lignin accounts for around 20% of the total liquids from fast pyrolysis of wood [34]. It can be seen in the GC results of Branca et al. [25] that the product composition from slow and fast pyrolysis is similar, except for the water content, which is higher in slow pyrolysis. Therefore, a similar but lower value of pyrolytic lignin in liquids from slow pyrolysis (15% of total condensable species) is assumed for this study.

Table 4
Comparison between experimental and model product compositions, for the original and adapted model with $x = 0.3$ for all components. Values in mass percentage of initial dry biomass.

	Branca et al. [25] 527 °C			Mihle et al. [26] 375 °C			Mihle et al. [26] 475 °C		
	Exp.	Orig.	Adap.	Exp.	Orig.	Adap.	Exp.	Orig.	Adap.
LIG_CC		0.61	0.60		1.98	1.98		0.01	0.01
G_CO2		0.37	0.26		1.06	0.75		0.00	0.00
G_CO		0.00	0.00		1.64	1.58		0.00	0.00
G_COH2		4.84	3.77		4.88	3.91		5.36	4.24
G_H2		0.09	0.11		0.12	0.10		0.13	0.10
Char (C)		7.45	18.19		8.08	18.42		9.62	19.98
Total solid	24.00	13.35	22.93	30.27	17.76	26.75	27.36	15.12	24.33
Hydrogen		0.00	0.40		0.00	0.38		0.00	0.40
Carbon monoxide		4.00	4.39		5.91	4.42		3.76	4.33
Carbon dioxide		10.00	8.80		12.48	5.73		8.26	11.22
Methane		0.50	2.23		2.27	0.42		2.42	2.24
Ethylene		<0.1	1.96		1.70	0.08		2.15	1.74
Ethane		<0.1			0.08			0.19	2.64
Total permanent gas	14.50	17.39	22.77	10.77	16.59	19.91	18.80	22.75	23.37
Water vapor	21.00	3.51	15.52	15.67	3.47	15.15	17.24	4.10	15.54
Formaldehyde		3.80	3.07		3.81	2.80		4.05	2.86
Acetaldehyde		0.20	1.80		0.22	1.76		1.00	1.86
Propanal/acetone		1.48	3.60		1.62	3.65		2.64	3.78
Methanol		3.01	2.74		3.19	2.75		3.48	2.90
Ethanol		1.12	0.94		1.15	0.85		1.20	0.85
Hydroxyacetalddehyde/acetic acid		0.93	11.43		0.97	11.08		5.06	11.08
Glyoxal		0.24	2.91		0.25	2.82		1.29	2.82
Propanedial		0.09	0.06		0.05	0.03		0.24	0.17
Exp. GC detected	10.17			23.15			9.52		
Exp. not detected	11.53			4.37			6.71		
Total carbonyls + alcohols	21.69	10.86	26.55	27.52	11.26	25.75	16.23	18.95	26.33
5-Hydroxymethyl-furfural		0.51	6.32		0.54	6.13		0.34	
Exp. GC detected	0.91			0.43			2.79		
Exp. not detected	5.14			4.37			6.71		
Total furans	6.06	0.51	6.32	4.81	0.54	6.13	7.05	2.79	6.13
Levoglucosan		0.66	40.92		0.70	39.98		3.83	30.08
Xylose monomer			5.17		0.00	1.57		0.00	0.39
Total sugars	0.66	46.08	0.00	0.70	41.55	0.00	3.83	30.47	0.00
Paracoumaryl alcohol		0.41	0.36		0.49	0.46		0.83	0.71
Phenol		0.19	0.17		0.24	0.23		0.38	0.33
Sinapaldehyde			7.70		5.39		8.10		4.61
Exp. 1 ring	2.86			0.83			1.18		
Exp. pyrolytic lignin	9.23			8.85			8.08		
Total phenolic	12.09	8.30	5.92	9.67	8.83	6.33	9.26	5.82	4.30
Total BTX/PAH	0.00	0.00	0.00	0.60	0.00	0.00	0.23	0.00	0.00

The rest of non-detected liquids, i.e. the liquids that are not water, pyrolytic lignin or were already detected by GC, belong to two categories:

- Non condensed liquids: In Branca et al. [25], it is reported that 6.38% of the total initial dry biomass is converted to not condensed liquids. It will be assumed that they correspond to the group “carbonyls + alcohols”. As they do not condense, they should have a low boiling point, as many of the components of this group, and none of others. In Milhe et al. [26], it is reported that all products were condensed, closing the mass balance. Actually, it can be noticed that components from this group (“carbonyls + alcohols”) with low boiling point, as formaldehyde, acetaldehyde or methanol, were detected in Milhe et al. [26] by GC and not in Branca et al. [25].
- Condensed but not detected liquids: The compounds not detected by GC, and that are not water or pyrolytic lignin, are assumed to be 50% from the group “carbonyls + alcohols” and 50% from the group furans. These compounds could not be detected because each species is present at very low concentrations. But as many species are present, the sum of the concentrations of all these species can be a relevant amount. In a detailed characterization of bio-oil from fast pyrolysis of beech from Azeem et al. [35], compounds with a concentration lower than 1% amount to 4.8% of the total mass. 2.4% of the total mass corresponds to furans and another 2.4% to the group “carbonyls + alcohols”. The proportion of each group from the mass that was not detected is taken from this study (50% “carbonyls + alcohols”, 50% furans), where a more detailed characterization is available. It is in principle possible that some sugars are also present, but considering the low amount of the most abundant one (levoglucosan, detected by GC) the amount of other sugars may be quite low.

3.2. Discussion

It can be seen in the comparison between the original scheme and the experimental data that there are some major deviations. Most of these deviations are corrected with the adapted scheme, as seen in Fig. 2. Related to the solid yield, the original scheme predicts a very low final solid yield, while the predicted solid yield is much better with the adapted scheme. The original scheme has a good prediction of the final solid yield in micro-TGA experiments, with a low amount of secondary charring reactions [24]. But in the evaluated experiments in this work, with the significant presence of secondary charring reactions, the final solid yield is better predicted by the adapted scheme, considering these charring reactions. Also from the experiments of Milhe et al. [26] the CHO composition of the final solid can be compared to the obtained values from the model, as shown in Table 5. The original scheme predicts a very low C and high O content. This is due to the lower amount of pure char (assumed as pure C in the scheme) than the G{} forms and remains of lignin. In the adapted scheme more pure char is produced through the secondary charring reactions, improving not just the prediction of the char yield, but also the C content of the final solid. The prediction of the O content also improves but the H content of the adapted scheme is under-predicted.

Additionally, the predicted yields of the carbonyls + alcohols, sugars and water vapor groups are significantly improved, as can be clearly seen in Fig. 2. The inclusion of the secondary charring reaction leads to the improvement in the final solid and water yields, as these are the main products of these reactions. A good prediction of the water yield is especially relevant due to the very different properties of water and other condensable species, as for heat of combustion. It should be noted that water corresponds to pyrolysis water and is not related to drying.

Also the elimination of the competition between sugars formation and fragmentation pathways in the cellulose and hemicellulose schemes lead to an improvement in the total yield of sugars, now not produced, and carbonyls + alcohols, which are the main products of these fragmentation reactions. It can be seen in the experimental data that sugars are produced in very low quantities in these conditions, so the assumption of neglecting its production seems reasonable.

The prediction of the total permanent gases is higher than in experiments for both the original and the adapted scheme (see Table 4). Comparing the individual species, it can be seen that hydrogen, methane and ethylene yields are over-predicted. Over-prediction of the yields of permanent gases as hydrogen and underprediction of the H content of the char may be related. Some of the hydrogen which is released in the model may be retained in the char at the current conditions. The yield of carbon monoxide is well predicted in Branca et al. [25] and in Milhe et al. [26] for the low temperature experiment (375 °C). In the experiment from Milhe et al. [26] at 475 °C, this yield is under-predicted. The reason may be that in this experiment there should be some tar cracking reactions, which produce mainly CO. In Branca et al. [25] a higher final temperature is achieved, but it is a batch process and most of the volatiles are released at temperatures lower than 400 °C. But in Milhe et al. [26] the volatiles go through a bed of char, which acts as a catalyst, at this temperature of 475 °C. So the extra CO produced by the secondary tar cracking reactions may be a reason for this deviation. The yield of carbon dioxide is well predicted in Branca et al. [25], but not in the experiments of Milhe et al. [26], where it is over-predicted. It is difficult to know what may be the reason of the different CO₂ yields.

The total “carbonyls + alcohols” group yield is correctly predicted in the experiment of Branca et al. [25] and Milhe et al. [26] at 375 °C by the adapted scheme, and somehow over-predicted in Milhe et al. [26] at 475 °C, probably due to the presence of secondary tar cracking reactions in this experiment, where the different compounds crack and produce CO and other components, as previously explained. It is difficult to compare the experimental yields of total furans, as these values depend on the assumption that 50% of the non GC detected volatiles are furans. With this assumption, which is uncertain, the experimental values are also close to the ones of the adapted scheme. Related to the phenolics, the total yields are under-predicted, but again the experimental value is uncertain due to the hypothesis that pyrolytic lignin represents 15% of the total condensable species. The current schemes do not predict the formation of BTX or PAH, that are detected by Milhe et al. [26]. These compounds are produced in secondary reactions [31,36] and could be included in future improvements of the scheme, but they represent a low amount of mass in these experiments.

Finally, the influence of variations of the “x” parameter on the predictions of the adapted model is checked. In Table 6 and Fig. 3 the results of the adapted model with different “x” values are presented and compared to the original scheme and the experimental results of Branca et al. [25]. “x” is kept constant for all reactions in all cases. When the “x” parameter increases, the yield of total solids and water vapor also increases, as these are the main products of the charring reactions. On the other hand, the yields of the groups of “permanent gases”, “carbonyls + alcohols”, “furans” and “sugars” decrease, as these are the main reactants of the charring reactions. It is not easy to define the optimal “x” parameter, as the increase of the parameter has contrary effects on the predictions. The value of 0.3 was previously proposed as it gives the best predictions for the total solid and volatiles yields. In Table 6 the averaged error for all product groups is shown for each model. The adapted model with “x = 0.4” has the lowest averaged error (<3%w.t.). In comparison to “x = 0.3”, groups as permanent gases

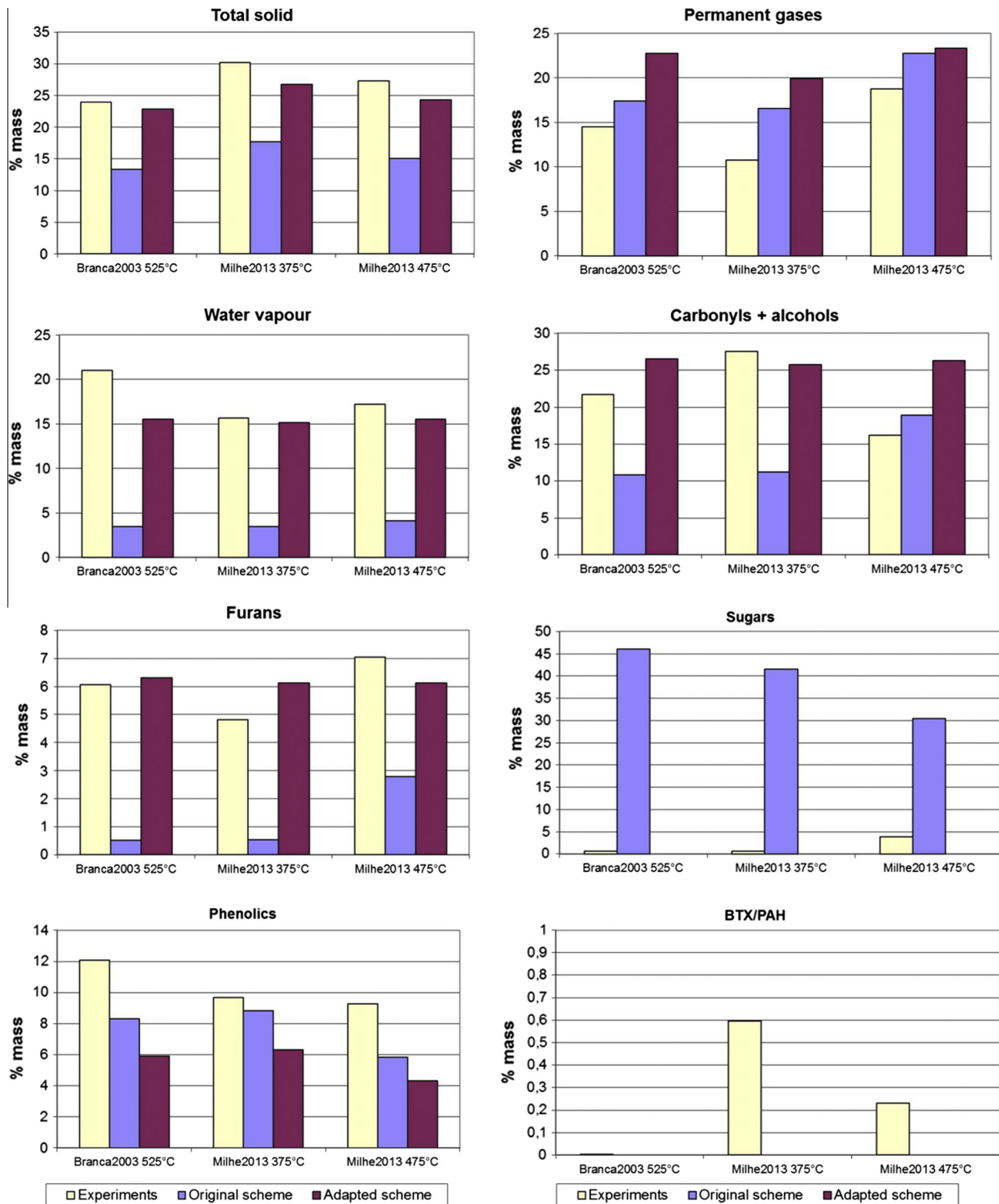


Fig. 2. Comparison between the measured mass yields in percentage of initial dry biomass of the main groups and the predicted values by the original and adapted scheme, with $x = 0.3$ for all reactions.

and “carbonyl + alcohols” are better predicted, but the total solid yield is overpredicted. Therefore, a value of “ x ” in the range 0.3–0.4 is recommended for the current conditions, i.e., slow pyrolysis in a fixed bed reactor with particles in the cm range of woody biomass. The ash content of the samples is in the usual range of woody biomass (without bark) [37,38]. Moreover, it should be stated that there is a lack of comprehensive analysis of product composition of fixed-bed pyrolysis in the literature. Assumptions were done to

estimate the amount of pyrolytic lignin and not GC detected furans and “carbonyl + alcohols”. A detailed characterization of fixed-bed pyrolysis products including these groups would be highly valuable in order to have a more detailed evaluation.

In solid fuels the volatile content is usually determined following the DIN-51720 norm, heating 1 g of solid fuel to 900 °C during 7 min. For the pine wood chips of Milhe et al. [26], the sum of fixed carbon and ash yields is equal to 16.7% d.b. The char yield obtained

Table 5

CHO mass content of produced char on dry ash free basis.

		% C	% H	% O
Milhe2013 375 °C	Experimental	82.01	4.17	13.82
	Original	69.86	3.11	27.03
	Adapted	83.19	1.75	15.06
Milhe2013 475 °C	Experimental	91.72	3.07	5.21
	Original	77.83	3.25	18.92
	Adapted	89.12	1.57	9.31

in the previously presented experiments is 27.36% at 475 °C. At 900 °C, a lower char yield would be obtained, but probably still higher than the sum of fixed carbon and ash yields. The reason is that in the employed fixed bed setup of the experiments of Milhe et al. [26] secondary reactions are enhanced to a greater extent than in the setup recommended by the DIN norm for the proximate analysis. Therefore, the proximate analysis is useful to compare the fixed carbon and ash yields of different fuels, but not to predict char yields, as these yields depend also on the amount of secondary reactions.

It has been shown that the adapted scheme can already provide a reasonably good prediction of product composition of pyrolysis in a fixed-bed reactor with particles of size in the order of 1 cm of woody biomass, although the “x” parameter representing secondary charring reactions was assumed to be constant for all reactions. Other limitation of the current scheme is that, although it is a mechanistic scheme and based on plausible decomposition mechanisms, it is still a simplified scheme and the real pyrolysis mechanisms are still unknown. The influence of the interactions between different biomass components is not considered, neither the extractives are considered. The effects of minerals are taken into account to some extent. However, considering these

limitations, the predictions are precise enough and the scheme is very valuable to predict the product composition of pyrolysis of biomass with the presence of secondary charring reactions, as in many practical applications, when the initial composition of lignocellulosic biomass is known. Other residues as plastics or sewage sludges [39,40] are not yet considered. The presented scheme provides significant advantages in contrast to the schemes that are currently being employed, where for example very different products as water and other condensable species are lumped in a group.

4. Conclusions

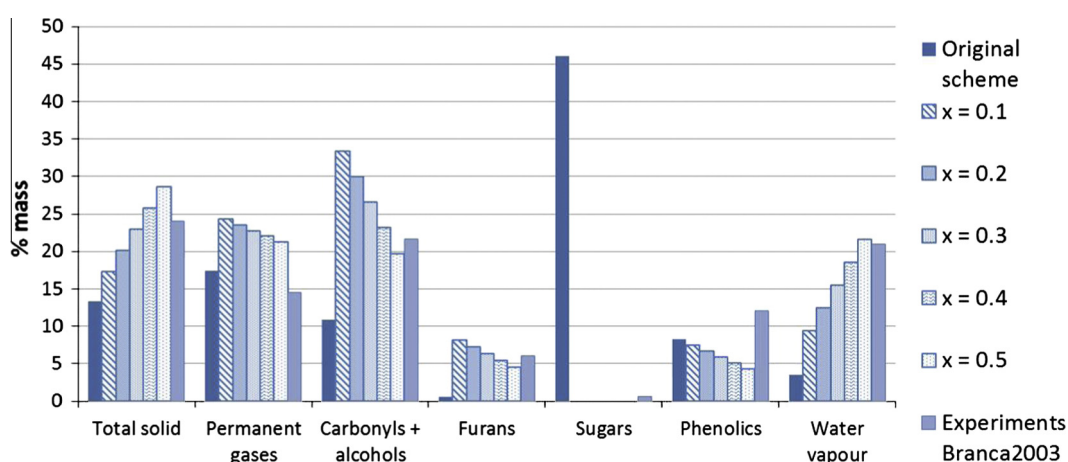
An adaptation of the mechanistic pyrolysis scheme developed by the group Ranzi for pyrolysis of small ash free biomass particles is proposed. Secondary char formation reactions, which are relevant for particles of a certain thickness, are included. Moreover, the catalytic effect of alkali metals in biomass is considered, which avoids sugar formation. The predictions of the adapted scheme are compared to experimental data from the literature. It is shown that it leads to a significant improvement in the predictions of the yields of the main volatiles groups and final char yield as well as its CHO composition.

A parameter “x” which determines the contribution of the secondary reactions for each biomass component is included in the adapted scheme. A general value in the range 0.3–0.4 for all components is proposed in this work for typical fixed-bed conditions, i.e., slow pyrolysis with particle size of about 1 cm of woody biomass. Future work should focus on the determination of the “x” parameter. A more precise scheme would have a different parameter for each component which depends on the pyrolysis conditions, e.g., heating rate, pressure, particle size, etc and content of inorganics. Pyrolysis experimental data of each biomass

Table 6

Comparison of the predictions of the adapted model in mass percentage with different “x” values, constant for all reactions in each case, with the experiments of Branca et al. [25].

	Experiments Branca2003	Original scheme	Adapted scheme				
			x = 0.1	x = 0.2	x = 0.3	x = 0.4	x = 0.5
Total solid	24.0	13.4	17.3	20.1	22.9	25.8	28.6
Total volatiles	76.0	86.6	82.7	79.9	77.1	74.2	71.4
Permanent gases	14.5	17.4	24.3	23.5	22.8	22.0	21.3
Carbonyls + alcohols	21.7	10.9	33.4	30.0	26.5	23.1	19.7
Furans	6.1	0.5	8.1	7.2	6.3	5.4	4.5
Sugars	0.7	46.1	0.0	0.0	0.0	0.0	0.0
Phenolics	12.1	8.3	7.5	6.7	5.9	5.1	4.3
Water vapor	21.0	3.5	9.4	12.5	15.5	18.6	21.6
Error (%)	0.0	13.4	6.7	5.1	3.5	2.9	3.6

**Fig. 3.** Comparison of the predictions of the adapted model with different “x” values, constant for all reactions in each case, with the experiments of Branca et al. [25].

pseudo-component and at different conditions would be required for this improvement. More detailed pyrolysis schemes for each pseudo-component and the interactions among them could be also investigated. Moreover, in the current scheme homogeneous tar cracking reactions of the volatiles species, which would occur at temperatures higher than 500 °C, are not included and should also be investigated.

References

- [1] Anca-Couce A, Zobel N, Jakobsen HA. Fuel 2013;103:773–82.
- [2] White JE, Catallo WJ, Legendre BL. J Anal Appl Pyrol 2011;91:1–33.
- [3] Di Blasi C. Prog Energy Combust 2008;34:47–90.
- [4] Kwiatkowski K, Gorecki B, Korotko J, Gryglas W, Dudynski M, Bajer K. Numer Heat Tr A – Appl 2013;64:216–34.
- [5] Miller R, Bellan J. Combust Sci Technol 1997;126:97–137.
- [6] Vinu R, Broadbelt LJ. Energy Environ. Sci. 2012;5:9808–26.
- [7] Mayes HB, Broadbelt LJ. J Phys Chem A 2012;116:7098–106.
- [8] Klein MT, Virk PS. Energy Fuels 2008;22:2175–82.
- [9] Faravelli T, Frassoldati A, Migliavacca G, Ranzi E. Biomass Bioenerg. 2010;34:290–301.
- [10] Ranzi E, Cuoci A, Faravelli T, Frassoldati A, Migliavacca G, Pierucci S, et al. Energy Fuels 2008;22:4292–300.
- [11] Piskorz J, Radlein D, Scott D, Czernik S. J Anal Appl Pyrol 1989;16:129–42.
- [12] Antal M, Varhegyi G. Ind Eng Chem Res 1995;34:703–17.
- [13] Mamleev V, Bourbigot S, Le Bras M, Yvon J. J Anal Appl Pyrol 2009;84:1–17.
- [14] Patwardhan PR, Satrio JA, Brown RC, Shanks BH. Bioresour Technol 2010;101:4646–55.
- [15] Lin Y-C, Cho J, Tompsett GA, Westmoreland PR, Huber GW. J Phys Chem C 2009;113:20097–107.
- [16] Banyasz J, Li S, Lyons-Hart J, Shafer K. J Anal Appl Pyrol 2001;57:223–48.
- [17] Milosavljevic I, Oja V, Suuberg E. Ind Eng Chem Res 1996;35:653–62.
- [18] Varhegyi G, Jakab E, Antal M. Energy Fuels 1994;8:1345–52.
- [19] Mamleev V, Bourbigot S, Yvon J. J Anal Appl Pyrol 2007;80:141–50.
- [20] Jensen A, Dam-Johansen K, Wojtowicz M, Serio M. Energy Fuels 1998;12:929–38.
- [21] Gomez CJ, Meszaros E, Jakab E, Velo E, Puigjaner L. J Anal Appl Pyrol 2007;80:416–26.
- [22] Varhegyi G, Antal M, Szekely T, Szabo P. Energy Fuels 1989;3:329–35.
- [23] Anca-Couce A, Berger A, Zobel N. Fuel 2014;123:230–40.
- [24] Frassoldati A, Migliavacca G, Crippa T, Velata F, Faravelli T, Ranzi E. In: Proceedings of the 29th meeting of the Italian Section of the Combustion Institute; 2006, section IX – 3.
- [25] Branca C, Giudicianni P, Di Blasi C. Ind Eng Chem Res 2003;42:3190–202.
- [26] Milhe M, van de Steene L, Haube M, Commandre J-M, Fassinou W-F, Flamant G. J Anal Appl Pyrol 2013;103:102–11.
- [27] Stengos T. ECON *4640 Applied Econometrics Course Notes. University of Guelph, 28 March 2003. Lecture Notes.
- [28] Di Blasi C, Signorelli G, Portorocco G. Ind Eng Chem Res 1999;38:2571–81.
- [29] Gomez-Barea A, Leckner B. Prog Energy Combust 2010;36:444–509.
- [30] Boroson M, Howard J, Longwell J, Peters W. Energy Fuels 1989;3:735–40.
- [31] Zobel N, Anca-Couce A. Proc Combust Inst 2013;34:2355–62.
- [32] Boroson M, Howard J, Longwell J, Peters W. AIChE J 1989;35:120–8.
- [33] Morf P, Hasler P, Nussbaumer T. Fuel 2002;81:843–53.
- [34] Bayerbach R, Meier D. J Anal Appl Pyrol 2009;85:98–107.
- [35] Azeez AM, Meier D, Odermatt J, Willner T. Energy Fuels 2010;24:2078–85.
- [36] Dieguez-Alonso A, Anca-Couce A, Zobel N. J Anal Appl Pyrol 2013;102:33–46.
- [37] Vassilev SV, Baxter D, Andersen LK, Vassileva CG, Morgan TJ. Fuel 2012;94:1–33.
- [38] Gronli MG, Varhegyi G, Di Blasi C. Ind Eng Chem Res 2002;41:4201–8.
- [39] Cepeliogullar O, Putun AE. Energy Convers Manage 2013;75:263–70.
- [40] Fan H, Zhou H, Wang J. Energy Convers Manage 2014 [in press]. <http://dx.doi.org/10.1016/j.enconman.2014.05.043>.
- [41] Blondeau J, Jeanmart H. Biomass Bioenerg 2012;41:107–21.